The correct citation for the paper is:

Cremaschi, L., and E. Lee. 2008. Design and heat transfer analysis of a new psychrometric environmental chamber for heat pump and refrigeration systems testing. *ASHRAE Transactions* 114(2):619-631.

Design and Heat Transfer Analysis of a New Psychrometric Environmental Chamber for Heat Pump and Refrigeration Systems Testing

Lorenzo Cremaschi, PhD
Associate Member ASHRAE

Edwin Lee
Student Member ASHRAE

ABSTRACT

This paper presents the design and heat transfer calculations of a new psychrometric environmental control climate chamber for heat pump and refrigeration systems testing. First, the standards for rating air conditioning and refrigeration systems are used to determine layout and floor area of the chamber. Then, a heat transfer model is developed to estimate the heat gain from the surrounding into the climate control chamber when the interior conditioned space is at temperature below freezing. The model, which was validated with data from the literature, also computes the wall thickness that would prevent water vapor condensation and subsequent accumulation on the outside walls of the facility. The results show that if the interior room temperature is below –20 °F (–28.9 °C), the thickness of the walls of the chamber ranges between 4 to 5 inches (10.2 to 12.7 cm), depending upon the thermal conductivity of the insulation panels. The outcomes of this paper also suggest that the cooling capacity of the conditioning system should be slightly oversized with respect to the capacity of the testing equipment inside the chamber. The additional capacity compensates for the heat transfer gained from the surrounding to the interior of the chamber, which is driven by the large temperature difference during testing at temperature below –20 °F (–28.9 °C).

INTRODUCTION

A psychrometric environmental control climate chamber consists of air conditioned rooms in which temperature, humidity, and airflow are controlled over a wide range of conditions with and without the addition of a live load. A live load, often referred as testing equipment, is a heat pump, an air conditioner, or a refrigeration system that runs inside the chamber at operating conditions similar to the ones it would have during its life of service. One room of the facility is used to artificially reproduce the outdoor environmental climate while the other room is employed to simulate the indoor environment [1].

The type of research testing in a university laboratory, as opposed to production testing, requires a unique design of the psychrometric chamber. The room is slightly oversized with respect to the dimensions of the testing equipment because instrumentation may have to be modified, calibrated, and improved in an iterative fashion. It is also necessary that the chamber be able to accommodate additional measurements, which might be redundant for an industrial production test psychrometric facility. This redundancy requires additional instrumentation such as mass flow meters, nozzles, anemometers, and dew point meters, which provide useful insight for the energy analysis of the testing system at design and off-design operating conditions. They also allow quantifying the performance and limitations of the testing equipment during dynamic transient periods, such as frosting and defrosting phases, cycling, and part load runs. To save cost, the psychrometric chamber at Oklahoma State University (OSU) is designed as two nearly identical rooms attached next to each other and they simulate a range of environmental conditions summarized in Table 1. The temperature of the outdoor climate chamber ranges from –40°F to +130°F (–40°C to +54.4°C), which is commonly used in research for heat pump and refrigeration components technology development [2-4]. This temperature range also applied to the fields of psychrometric at freezer temperatures [5, 6], industrial, storage, and transport refrigeration [7, 8], heat pump systems performance rating [9, 10], few cooling systems for military applications

Lorenzo Cremaschi is an assistant professor and **Edwin Lee** is a graduate research assistant in the School of Mechanical and Aerospace Engineering, Oklahoma State University, Stillwater, OK.

Table 1. Main Design Specifications of the Psychrometric Test Facility at Oklahoma State University

Parameter	Indoor Environmental Chamber	Outdoor Climate Control Chamber
Temperature	55°F to +100°F (13°C to 38°C)	–40°F to +130°F (–40°C to +54.5°C)
Relative humidity	20%RH to 90%RH	10%RH to 95%RH
Maximum capacity of the testing equipment	15 tons (52.7 kW) of refrigeration at 55°F (12.8°C)	15 tons (52.7 kW) of refrigeration at –40°F (–40°C)
Maximum airflow rate	8000 cfm (≈ 227 m^3/min)	8000 cfm (≈ 227 m^3/min)
Maximum weight of testing equipment	3000 lb (1361 kg)	3000 lb (1361 kg)
Dimensions	19 × 22 × 17 ft high (5.8 × 6.7 × 5.2 m)	22 × 22 × 17 ft high (6.7 × 6.7 × 5.2 m)
Pull-down rate when empty	N/A	from +78°F to –40°F in 5 hours (from 25.6°C to –40°C in 5 hours)

Table 2. Control Accuracy and Precision Criteria of the Psychrometric Test Facility under Standard Rating Conditions*

Indoor/Outdoor Chamber		
Parameter	**Accuracy Criteria**	**Precision Criteria**
Airflow rate	±3% of setpoint	±5% of mean
Relative humidity	±2%RH	±3%RH
Pressure	±1 Pa	±2 Pa
Temperature	±0.5°F (±0.27°C)	±0.9°F (±0.5°C)

* Standard ARI 210/240: "A" cooling steady-state conditions for air-cooled equipment [9].

[11, 12], and several cooling processes found in the petrochemical industry [13]. The control accuracy and precision of the psychrometric chamber are summarized in Table 2. Control accuracy is defined as the difference between the mean value of the parameter and its set point. Control precision is defined as the standard deviation of the parameter from its mean value. The values of Table 2 meet the ASHRAE standards [14-17] and they guarantee accurate and repeatable measurements within small uncertainty. They are commonly adopted in the scientific community of HVAC & refrigeration research [18, 19]. The close control of temperature and relative humidity is preserved even with the addition of a live load in the chamber and during dynamic on-off and defrosting cycles of the testing equipment.

Uniform airflow and temperature distribution inside the rooms are essential for high-quality research testing. If the room is too crowded, turbulence and stagnation areas are likely to occur. If this is the case, the experiments are not repeatable, the air side conditions are not well-defined, and the uncertainty on the measurements is significantly increased. These considerations suggest making the room larger and designing an air distribution system that provides a very uniform airflow independent of the position of testing equipment. The psychrometric chamber at OSU adopts raised perforated tiles to control properly the air velocity around the testing equipment. This approach is well known in air distribution systems of raised-floor data-centers [20, 21] and modern office buildings [22, 23]. Because of the extreme design conditions of the present psychrometric chamber, first a review of the most relevant ASHRAE and ARI standards is presented and the recent publications available in the open literature are reviewed. Then, a heat transfer analysis of the psychrometric chamber is discussed. The calculations of the heat gain from the surrounding into the climate chamber are presented and the wall thickness for proper insulation is addressed.

DETERMINATION OF THE DIMENSIONS AND LAYOUT OF THE CHAMBER BY USING THE ASHRAE/ARI STANDARDS

According to Table 1, the outdoor chamber is the most critical room because it is designed to operate in a broader range of temperature and relative humidity. The interior volume of the outdoor chamber accommodates a 15 ton (≈53 kW) of refrigeration rooftop unit, including sensors, transducers, and flow meters. During the testing of a 15-ton heat pump system, the estimated rejected heat from the unit can range from 20 to 25 tons, depending on the temperature of the heat sink medium and on the efficiency of the equipment. Thus, the chamber conditioning equipment needs to handle at least 25 tons of refrigeration. In addition, the refrigeration system of the facility must compensate for the heat gained from the surrounding into the outdoor climate chamber when it operates at low temperature conditions. The ambient for the psychrometric facility at OSU is assumed to be at constant temperature of 78°F (25.6°C) and 45% RH For the heat transfer analysis, the dry-bulb temperature and relative humidity of the indoor environmental chamber are set to 70°F (21.1°C) and 56% R.H, respectively, according to the ASHRAE and ARI standards for low temperature heat pump system performance testing [9, 14]. The radiant heat transfer effect is neglected because the facility construction site is located inside a building of the university campus.

Although it is desired to have a large floor area to allow multiple test setups inside the chamber, the total floor area of the chamber is limited by available space of the actual construction site, which is approximately 42 by 23 by 18 ft high (13 x 7 x 5.4 m). Since the facility is dedicated to heat pump systems testing, two nearly identical rooms separated by an internal wall are designed within the space available to save cost. The two rooms have internal footprint area of about 19 by 22 ft (5.8 x 6.7 m) and 22 by 22 ft (6.7 x 6.7m) for the indoor and outdoor environmental space, respectively. It is assumed that at least two units are set up inside each room for testing and calibrating procedures. One example showing a possible layout of two units in the outdoor room is given in Figure 1. One rooftop unit, whose dimensions are approximately 6 by 2.5 ft (1.8 x 0.8m), is placed into the room and it is the primary equipment. A second unit is set up, instrumented, and modified during the periods in which test data are not recorded. The second unit ultimately standbys awaiting testing. In order to be conformed with the Standard 37 [14], any surface that discharges air must be placed at least 6 ft (1.8m) from any other surfaces in the room. Secondly, surfaces on the test unit other than air discharge surfaces must be at least 3 ft (0.9m) from all other room surfaces. To be consistent with the Standard 41.2 [15], the converging duct should have a convergence angle of no more than 7.5°. Thus, an outdoor climate chamber of about 22 by 22 ft provides enough space to accommodate the equipment, airflow measurement devices, fans, data acquisition hardware, and personnel work space for set up and modification of the testing units.

When performing tests on heat pump systems, unitary, and refrigeration equipment, the standards dictate testing conditions, accuracy, data analysis, and data reduction methods. In the literature, several standards are relevant to establish a framework for the design of the present psychrometric chamber and a brief summary is given in Table 3. For each standard, the aspects that are pertinent to the present psychrometric facility design have been highlighted in the main content column. In the table, it has also been emphasized the information that is omitted in the standards and that would help with the design of a psychrometric HVAC simulator laboratory.

From the ASHRAE and ARI standards, it seems that there is a lacking of information about the conditioning equipment characteristics, its capacity safety factor, noise reduction techniques for structural vibration and refrigeration pipelines, heat resistance coefficient of poor to excellent insulation panels used in common HVAC simulators, air leak rate and its impact on the tests accuracy and repeatability. The standards specify that the airflow must be uniform around the testing equipment, but they do not propose any guideline about the air supply systems and diffuser configurations. In addition to provide basic guidelines for chamber operation, the standards might be improved by including few examples of sizing, load calculations, and air distribution systems that can be adopted in the design of a psychrometric chamber. It is clear that final design must be made based on the specific chamber application, available space, performance of the conditioning equipment, and financial budget. Ultimately, the experience in the field becomes the most important players during the design of a psychrometric chamber. Thus, a review of the relevant work in the existing literature is discussed in the next section.

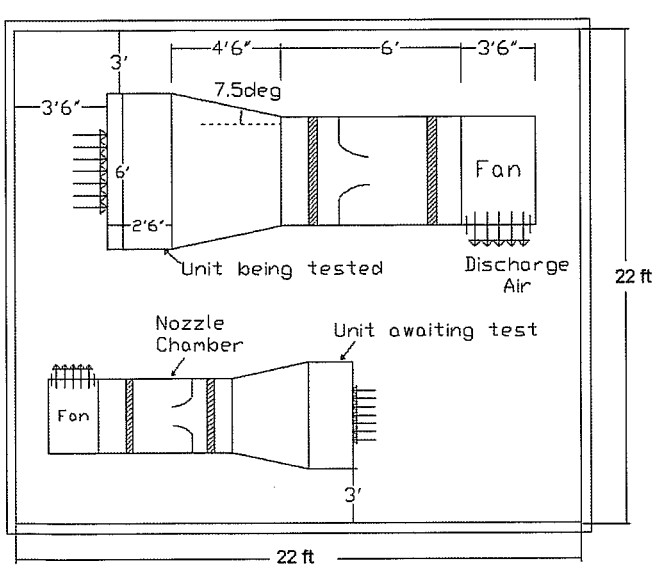

Figure 1 *Example of airflow measurement set up in the outdoor climate chamber.*

LITERATURE REVIEW OF PSYCHROMETRIC CHAMBER DESIGNS

Chatzidakis et al. [24] proposed a numerical study of an environmental chamber that was utilized to perform test measurements of food refrigeration in transportation systems. The purpose of the study was to develop an improved controls strategy for the environmental chamber, and to investigate the sensitivity of pull down rates with respect to floor slab thickness of the chamber. The test measurements required that steady state be held for at least twelve hours, so higher pull down rate would decrease the overall testing time, and consequently, the testing costs. Their analysis showed that the pull down rates decreased by up to 10% with different thicknesses of concrete floor, varying from 3.9 to 11.8 inches (10 to 30 cm). The results of their work suggested that the thickness of the insulation panels is crucial to decrease pull down soaking time.

A small psychrometric test chamber, developed for instructional purpose, is discussed in a paper by Swedish [25]. The chamber dimensions were 8 by 4 by 9 ft high (2.4 x 1.2 x 2.7 m), and it had a single supply and return air diffuser. The entire chamber conditioning equipment was assembled inside in the air return duct. The components of the conditioning equipment included a fan, cooling unit, strip heaters, water sprayers, and temperature, pressure, and flow meter sensors. The chamber was used to demonstrate fundamental psychro-

Table 3. Summary of the Standards Used for the Design of the Psychrometric Chamber at OSU

Standard	Year	Title	Main Content	Would Like More Information on
ASHRAE Standard 37 [14]	1988 and 2005 update	Methods of Testing for Rating Unitary Air-Conditioning and Heat Pump Equipment	- equipment type - accuracy requirements - layout diagrams - calculation methods - test procedures	- soaking time - wall thickness - insulation methods - room airflow configuration - test conditions, accuracy, and precision at extreme high/low temperatures
ASHRAE Standard 40 [17]	1980 and 1992 update	Methods of Testing for Rating Heat-Operated Unitary Air-Conditioning Equipment for Cooling	- how to include the heat loss from the flue gas	
ASHRAE Standard 41.1 [16]	1986 and 1991 update	Standard Method for Temperature Measurement	- methods to measure the temperature in both steady state and transient operations from –40°F to 400°F (–40°C to 204°C) - how to construct air-stream mixing devices and air sampling devices	- how sensors location in the climate chamber affect the uncertainty and repeatability of the measurements
ASHRAE Standard 41.2 [15]	1987 and 1992 update	Standard Methods for Laboratory Airflow Measurement	- pitot-static tubes - nozzles measurement devices	- guidelines to define the floor area of psychrometric chamber - effect of the height of the chamber
ARI 210/240 [9]	2005	Performance Rating of Unitary Air-Conditioning and Air-Source Heat Pump Equipment	- test conditions for different equipment types - data analysis and data reduction - nameplate information - tunnel air testing method	- structural and load calculations for the chamber based on the dimension of the testing equipment - capacity safety factors for the space and conditioning equipment - layout of air diffusers and air return grids
ARI 340/360 [10]	2004	Performance Rating of Commercial and Industrial Unitary Air-Conditioning and Heat Pump Equipment		

metric processes and the control of the chamber was capable of holding the dry bulb temperature to within 1°F (0.6°C) and relative humidity to within 2%. The test cell presented in Swedish's work is dedicated to very small HVAC applications and the temperature range was from 40°F to 101°F.

Environmental control cells in industrial food refrigeration facilities share most of the design traits with the psychrometric chamber of the present work. Sando and Abdou [26] discussed the selection of a prepackaged commercial unit cell and the design of a customized unit cell. Usually customized units control air temperature, humidity, and velocity and they do not have floor drains to minimize the air leak and infiltration. In their paper it was reported that a typical unit for temperature ranging from –50 to 100°F (–45.5 to 37.7°C) had urethane-insulated metal-covered screed around the perimeter of the cell to receive the bolts of the vertical wall panels. The overall heat transfer coefficient, U, was about 0.0295 Btu/hr-ft^2-°F (0.167 W/m^2-K), which is one of the lowest (and therefore one of the best) wall material used in industry today. However, Sando and Abdou pointed out that this U-value cannot be used by the designer for the entire wall in a heat gain/loss calculation because of the thermal bridges occurring where the panels are joined together. The large temperature difference between the test cell and the ambient temperature might cause a rapid heat transfer rate and special sealing material and assembly techniques are required to stop leakage from test cell panel joints. They also stated that cooling of the chamber is performed by mechanical refrigeration (vapor compression) systems, and heating is usually done by electric heat, except where other means are required by the application. As pointed out by Berchtold [27], most of the low temperature environmental testing is done at –40°F (–40°C), and a cascaded multi-stage refrigeration system might be necessary to achieve this temperature. Particular care must be paid to the size of the conditioning equipment in relation to the testing units because any unnecessary oversize of the chamber conditioning equipment results in very high cost penalization. Berchtold reported that pull-down rates of environmental chamber available on the market were as high as 27°F/min (15°C/min). He also observed that with drastic temperature changes, expansion and contraction of the refrigerating pipelines might occur, especially if the wall separates a cold space from a hot space. A secondary aspect was the noise due to the

mechanical equipment and piping vibration, which should be in the range of 70dB to 80dB [28].

The observations from the open literature about structural stress, vibration, heat losses, and conditioning equipment were collected and used to compile a preliminary financial budget for the current facility. The cost of a food refrigeration industrial test cell [26] are compared with the estimated costs of the current psychrometric environmental climate control chamber at OSU. It appears that the psychrometric chamber of this work is more weighted heavily toward the structural fabrication as it is shown in Figure 2. The structural part includes chamber design, site preparation, transportation of the panels, assembly, and fire protection system. The mechanical part includes conditioning equipment, instrumentation and data acquisition hardware, and the electrical part consists mainly of controls and data acquisition software. The estimated expenses for the present chamber are more weighted for the structure of the facility because the chamber is slightly oversized compared to commercial test cells, it includes a raised-floor air distribution system for better airflow control, and the insulation panels are completely customized for the extreme range of temperature of this application.

Although there are several work in the literature that describe qualitatively the design of a psychrometric chamber, few methods have been found that estimate the energy loads in a structure with cooling and heating load profiles similar to the ones of the present work [29, 30]. Despite the large effort expended on estimating the load calculations of office buildings and residential homes [31, 32], the aim of the present study is to explore the possibility of a simpler and more physical approach to find the heat transfer loss/gain through the structure of the psychrometric chamber. Finite element numerical methods required specialized expertise, which are usually application-oriented and specific to the structural framework of the environment and the activities it support [33]. They also require a level of knowledge about material, configuration, layout, and dimensions, which often are not know at the early stage of the design. From the outcomes of the present work, the main dimensions of a psychrometric facility are defined in relation to the temperature range of the climate chamber and cooling capacity of the testing equipment. Once the chamber layout, panel thickness, and heat losses are estimated with the model developed in the present work, more sophisticated numerical finite element approaches can be used for further refinements and optimization, i.e., minimization of the energy losses and reduction of the initial capital investment of the chamber.

HEAT TRASNFER MODEL FORMULATION FOR THE PSYCHROMETRIC CHAMBER

The geometry of the outdoor climate control chamber resembles a rectangular box and it is divided into six surfaces: the floor, the ceiling, two side walls, one front wall, and one intermediate wall of separation from the indoor environmental room. A control volume approach is chosen for each section to analyze the heat transfer processes through the structure and within the boundary layers near the surfaces. The model is based on fundamental thermodynamic and heat transfer laws [34, 35] and it relays on experimental thermal conductivity data of the panels [36], which are joined together to form the walls, ceiling, and floor of the chamber.

The heat transfer rate from the surrounding to the chamber, $\dot{Q}_{gain,tot}$, is calculated as sum of the heat transfer gained through each surface as follows:

$$\dot{Q}_{gain,tot} = \sum_{j=1}^{6} \dot{Q}_j \tag{1}$$

$$\dot{Q}_j = U_j \cdot A_{ht,j} \cdot \Delta T_{int-amb} \quad \text{for } j = 1 \text{ to } 6 \tag{2}$$

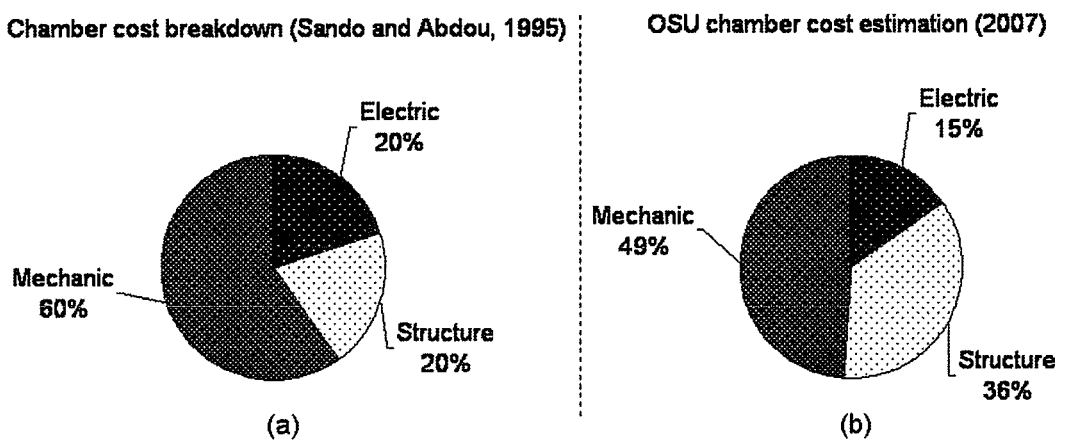

Figure 2 *Comparison between (a) costs of the facility presented by Sando and Abdou (1995) and (b) estimated expenses for the psychrometric chamber at OSU.*

where U_j and $A_{ht,j}$ are the average overall heat transfer coefficient and the heat transfer area of the surface j, respectively. The temperature difference, $\Delta T_{int\text{-}amb}$, is calculated between the ambient surrounding the chamber, T_{amb}, and the air in the interior of the climate room, T_{int}. In case of the intermediate wall of separation, the external ambient temperature is set to the dry-bulb temperature of the indoor environmental chamber, which is about 70°F (21.1°C). For each surface, the average heat transfer coefficient is calculated as follow:

$$\frac{1}{U_j} = \left(\frac{1}{\bar{h}_{out,j}} + \frac{t_{panel,j}}{k_{c,\,eff,\,i}} + \frac{1}{\bar{h}_{in,j}} \right) \tag{3}$$

where $\bar{h}_{out,j}$ and $\bar{h}_{in,j}$ are the average convective heat transfer coefficient of the film near the outside and inside surfaces of the panels forming the wall j. The effective thermal conductivity of the panel, $k_{c,eff,j}$, has been calculated based on the thickness of the panel, $t_{panel,j}$, material, side dimensions, and thermal bridge effect of the panels where they are joined together to form the wall j. The panels for the current psychrometric chamber consist of a sandwich structure similar to the one shown in Figure 3.

Each panel consists of two metal sheets (aluminum or steel) that bind an insulation expanded foam core region. At the edges of each panel two pieces of low-conductivity neoprene-based tape acts as a thermal break, separating the interior metal sheet from the side metal edge. This configuration reduces heat loss and thermal bridges where the panels are joined together. Additional advantages are transportability, easy to assembly, and resistance to compressive loads [36]. The thickness of a panel, t_{panel}, can vary between 2 to 6 inches (5.1 to 15.2cm) and the width of the panel, W_{panel}, can vary from 3 to 8 ft (0.9 to 2.4m), depending on the mechanical stress acting on the chamber structure, manufacturer capabilities, and cost of production. The thermal bridge at the metal sheet sides of the panel plays an important role in the heat transfer conduction analysis. It was shown that the thermal bridge increases the heat flux through the panel with respect to the ideal heat flux, which was calculated using the infinite plate assumption [36]. The effect of the sheet metal sides decreases if the panel width increases and the overall heat flux asymptotically approaches that of the infinite plate assumption. The effective thermal conductivity of the panel used in the design of the current psychrometric facility accounts for the heat being transferred through the metal sheet sides. An empirical factor, F, which was provided by the panel manufacturer, is used in a 1D heat thermal conductivity equation as follows:

$$\frac{t_{panel,j}}{k_{c,\,eff,j}} = \frac{1}{(1+F)} \cdot \left(\frac{t_{met}}{k_{c,\,met}} + \frac{t_{foam}}{k_{c,foam}} \right) \tag{4}$$

where the geometric and material properties of the panels are given in Table 4.

It is assumed that the inside and outside surface temperature of each wall is uniform and the ground floor of the chamber is assumed adiabatic. The thermodynamic and heat

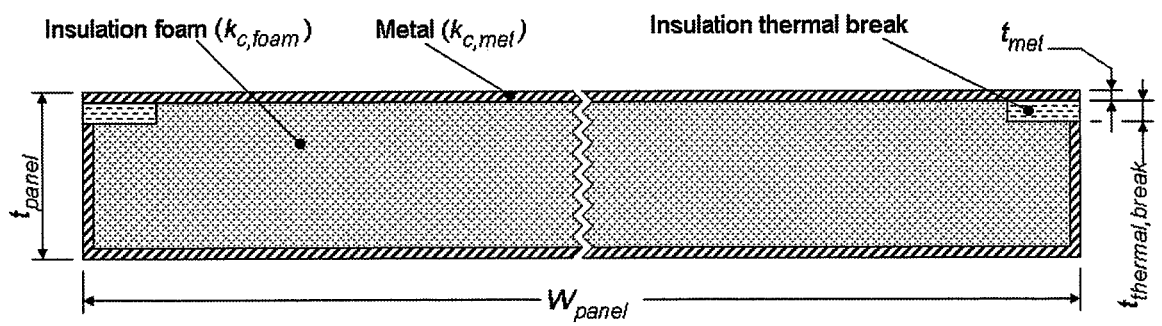

Figure 3 *Example of insulation panel for building air-conditioning systems.*

Table 4. Geometric and Material Properties of the Panels for the Psychrometric Chamber at OSU

		Variable	Value / Range
t_{met}	:	Metal sheet thickness	0.0175 in (~0.45 mm)
$t_{panel,j}$	:	Total thickness of the panel	From 2 to 6 in (5.1 to 15.2cm)
t_{foam}	:	Insulation foam thickness	$t_{foam} = t_{panel,j} - 2 \cdot t_{met}$
$k_{c,met}$	:	Thermal conductivity of the metal sheet	120 Btu-in/hr-ft^2-°F (17.3 W/m-°C)
$k_{c,foam}$	:	Thermal conductivity of the insulation foam [37]	0.019 Btu/hr-ft-°F (0.027 W/m-°C)

transfer properties are evaluated at the average film temperature corresponding to each surface j, defined as follows:

$$T_{film,in,j} = \frac{T_{int} + T_{s,in,j}}{2} \text{ and}$$

$$T_{film,out,j} = \frac{T_{amb} + T_{s,out,j}}{2}$$

$$\text{for } j = 1 \text{ to } 6 \tag{5}$$

where $T_{s,in,j}$ and $T_{s,out,j}$ are the temperatures of the inside and outside surface of the panel forming the wall j, ceiling, and floor, and they are calculated as follows:

$$T_{s,in,j} - T_{int} = \frac{1}{\bar{h}_{in,j}} \cdot \frac{\dot{Q}_j}{A_{ht,j}} \text{ and}$$

$$T_{s,out,j} - T_{amb} = \frac{1}{\bar{h}_{out,j}} \cdot \frac{\dot{Q}_j}{A_{ht,j}} \tag{6}$$

The convective heat transfer coefficient of the film have been calculated according to the correlations proposed by Homan [34] and Incroprera [35]. For each surface, the Nusselt number, Nu_j, was calculated according to the orientation (vertical for side, front, intermediate, and back walls; horizontal for floor and ceiling), Reynolds number, Re_j, Grashof number, Gr_j, and Prandtl number, Pr_j. These dimensionless numbers are calculated for each film region on the inside and outside the wall surface as follows:

$$Re_j = \frac{u_{\infty,j} \cdot L_j}{\nu_j}$$

$$Gr_j = \frac{g \cdot \beta_j \cdot (T_{s,j} - T_{\infty,j}) \cdot L_j^3}{\nu_j^2} \tag{7}$$

$$Pr_j = \frac{c_{p,j} \cdot \mu_j}{k_{air,j}} = \frac{\nu_j}{\alpha_j}$$

where ν is the kinematic viscosity of the film, g is the gravity acceleration, β is the inverse of the film absolute temperature ($\beta = 1/T_{film}$ [K^{-1}]), and c_p and k_{air} are the specific heat and thermal conductivity of the film, respectively. $T_{\infty,j}$ is the temperature of the air approaching the surface, that is, the ambient temperature or the interior temperature for the outside and inside film regions, respectively. The Nusselt number of each surface depends on its characteristic dimension, L_j, orientation, predominance of convection flow regime (forced versus free convection), film average temperature, temperature gradient in the film, and velocity, $u_{\infty,j}$, of the air approaching the surface. The Nusselt numbers are calculated according to the fundamental heat transfer correlations [34] in dimensionless form as summarized in the following equations and more in details in the Appendix:

$$Nu_{in,j} = \frac{\bar{h}_{film,in,j} \cdot L_{in,j}}{k_{air,in,j}}$$

$$= f(L_{in,j}, \text{orientation}_j, Re_{in,j}, Gr_{in,j}, Pr_{in,j}) \tag{8}$$

$$Nu_{out,j} = \frac{\bar{h}_{film,out,j} \cdot L_{out,j}}{k_{air,out,j}}$$

$$= f(L_{out,j}, \text{orientation}_j, Re_{out,j}, Gr_{out,j}, Pr_{out,j}) \tag{9}$$

It is assumed that natural convection circulation is established at the outer surfaces of the chamber since the ambient air is still (mean velocity $u_{\infty,amb} = 0$ mph) and the temperature gradient in the film drives the flow near the surfaces. The total volume flow rate of supply air into the outdoor chamber is 8000 cfm (3.7 m^3/s), which results in an air mean velocity inside the chamber of about $u_{\infty,int} = 0.2$ mph (≈0.1 m/s). The predominance of forced versus natural convection is determined upon the ratio of $Gr_{in,j}/Re^2_{in,j}$, in which $Gr_{in,j}$ and $Re_{in,j}$ are the Grashof number and Reynold number for film regions near the wall surfaces. Similarly, the air inside the indoor environmental chamber rises at about 0.2 mph and, depending upon the temperature gradient in the film region, the ratio of Gr/Re^2 determines the convection regime within the boundary layer near the surface of the intermediate separation wall.

The present model is implemented in EES (Engineering Equation Solver, [38]) and the system of Equations 1 to 9 is solved for panel thickness between 2 to 6 inches (5.1 to 15.2 cm), and for the interior temperature varying from $T_{int} = -40$ to 0°F (–40 to –17.8°C).

Model Validation

Before considering the simulation results and in order to show the appropriateness of the present approach, the model described above was compared with results from the available literature. First, the model was applied to several examples discussed in [32, 35] and the heat transfer rate was predicted within ±5% with respect to their analytical solutions. Then, the present model was validate against four references in the literature, which are more complex configurations and provide broader ranges for characteristic dimensions, temperature, air velocity, and application. The model was applied to the heat transfer analysis for actual refrigerator, freezers, enhanced insulation panels, and environmental chamber for transport refrigeration. The surface temperature and heat transfer rate from the current model were compared with those found in the reference and the comparison is summarized in Table 5. The details of the results from the references are given in [24, 39-41]. If we consider the average temperatures and heat transfer rates from the surrounding into the compartment it is concluded that the predictions from the present model are in satisfactory agreement with the data given in the references. Compared to experimental and numerical methods, the present model is less accurate but still able to capture the nature of the heat transfer process. It also predict the mean values of the surface temperature within ±3°F (±1.6°C), and the average heat transfer rate gained from the surrounding into the conditioned compartment is within ±41% with respect to the range given in the references. The discrepancies are due to the simplifying assumptions and 1-D approximations of the present control volume approach. However, the current model is

Table 5. Comparison of the Present Heat Transfer Model with References in the Literature

	Reference				Present Model			Error
	Application and Temperature of the Ambient (T_{amb}) and Interior (T_{int})	Conv. Type	Surface Temperature	Heat Gain from Surrounding	Conv. Type	Surface Temperature*	Heat Gain from Surrounding	ε_Q = Relative Error for Heat Transfer Rate;† ε_T = Error for Surface Temperature†
Case 1 [39]	Freezers compartment T_{amb} = 90°F; T_{int} = 5°F	—	$T_{s,out}$: — $T_{s,in}$: —	95 to 103 Btu/h	natural	$T_{s,out}$: 75°F to 84°F $T_{s,in}$: 5°F to 18°F	162 Btu/h	ε_Q = 36% to 41%
	Refrigerator compartment T_{amb} = 90°F; T_{int} = 45°F	—	$T_{s,out}$: — $T_{s,in}$: —	73 to 92 Btu/h	natural	$T_{s,out}$: 82°F to 89°F $T_{s,in}$: 45°F to 54°F	82 Btu/h	ε_Q = 11% to 12%
Case 2 [40]	Insulation panels for freezers / refrigerators; T_{amb} = 76.1°F; T_{int} = 0°F	—	$T_{s,out}$: 68°F to 73°F $T_{s,in}$: —	—	forced and natural	$T_{s,out}$: 68°F to 70°F $T_{s,in}$: 2°F to 6°F	—	ε_T = up to 3°F
Case 3 [41]	Freezers compartment T_{amb} = 84°F; T_{int} = –6.6°F	forced	$T_{s,out}$: — $T_{s,in}$: –1°F to 2°F	31 to 51 Btu/h	forced and natural	$T_{s,out}$: 62°F to 68°F $T_{s,in}$: –0.1°F to 3.7°F	44 Btu/h	ε_Q = 16% to 29% ε_T = 0.9°F to 1.7°F
	Refrigerator compartment T_{amb} = 84°F; T_{int} = 28.1°F	mixed	$T_{s,out}$: — $T_{s,in,}$: 35°F to 42°F	112 Btu/h	forced	$T_{s,out}$: 67°F to 70°F $T_{s,in}$: 33°F to 39°F	80 Btu/h	ε_Q = up to 40% ε_T = 2°F to 3°F
Case 4 [24]	Environmental chamber for transport refrigeration; T_{amb} = 77°F; T_{int} = 45.5°F	forced	$T_{s,out}$: — $T_{s,in}$: —	up to 10236 Btu/hr	forced	$T_{s,out}$: 68°F to 72°F $T_{s,in}$: 46°F to 48°F	4373 Btu/h (average value)	Average Q not available in the reference

* For the present model the result represents the mean temperature of the surface. The temperatures of the adiabatic surfaces are identical to the ones in the reference and they are excluded from the comparison.

† Error is calculate as follows: $\varepsilon_Q = \left|\dot{Q}_{reference} - \dot{Q}_{model}\right| / \dot{Q}_{model} \times 100$ and $\varepsilon_T = \left|T_{reference} - T_{model}\right|$.

simple but accurate enough to be useful during the preliminary design calculations of psychrometric chambers, refrigerating partitions, and freezing boxes in general.

DISCUSSION OF THE RESULTS

The present model is applied to the outdoor climate chamber of the psychrometric facility to estimate the heat gain into the chamber from the surrounding ambient when the interior temperature is at its minimum, that is, equal to –40°F (–40°C). The model is also used to determine the minimum thickness of the panels that would prevent water vapor condensation on the outer surfaces of the chamber. If the outer wall surface temperature drops below the dew point of the ambient air, water vapor in the air may condense and the droplets may infiltrate in the structure. This leads to water retention in the panels, which ultimately deteriorate the mechanical and thermal insulation properties of the chamber structure. Consequently, for proper design of the chamber, it must be ensured that if the chamber is cooled below freezing temperature, the panels provide sufficient insulation to prevent condensation on the outer (warm) wall surfaces.

The simulations were performed with panel thickness varying from 2 to 6 inches and panel side width from 3 to 8 ft. The average effective thermal conductivity of the panels resulted equal to $k_{c,eff}$=0.234 Btu-in/hr-ft^2-°F (0.034 W/m-°C) and the panel width was about 4 ft. If the width of the panel varies from 3 to 8 ft, the effective thermal conductivity of the panel changed of about ±10% from the average effective ther-

mal conductivity. The total heat transfer rate from the surrounding to the chamber varied from 5809 to 11503 Btu/hr (~1.7 to 3.4 kW) and the wall contribution was about 78% of the total heat transfer rate into the chamber. The heat transfer rate and surface temperatures of each section (walls, ceiling, floor, and intermediate separation wall) are given in Table 6.

The Prandtl number was about 0.75 for the cold film region on the interior side and 0.74 for the warm film region on the outside of the chamber structure. The dimensionless numbers, convective heat transfer coefficients, and overall average heat transfer coefficients depend on the orientation of the panels and they are summarized in Table 7. Due to the heat transfer characteristics of the psychrometric chamber the walls are usually colder than the ceiling and, thus, water vapor would condense preferably on the vertical walls rather than on the horizontal ceiling. The outside region of the chamber floor is the ground floor of the building, which was assumed adia-

Table 6. Heat Transfer Rate and Surface Temperatures of Each Section of the Psychrometric Chamber

	Heat Transfer Rate from Surrounding into the Chamber ($k_{c,eff}$ = 0.23 Btu-in/hr-ft^2-°F)	Surface Temperature (T_{amb} = 78°F and T_{int} = –40°F) ($T_{ind,env}$ = 70°F)
Ceiling	1368 – 2854 Btu/hr (~0.4 – 0.84 kW);	$T_{s,out}$ = 46 to 62°F; $T_{s,in}$ = –24 to –10°F
Floor	~ 0 Btu/hr	$T_{s,out}$ = 78°F; $T_{s,in}$ = –40°F
External wall	1130 – 2203 Btu/hr (~0.33 – 0.65 kW)	$T_{s,out}$ = 42 to 58 °F; $T_{s,in}$ = –21 to –5 °F
Separation wall	1049 – 2036 Btu/hr (~0.31 – 0.6 kW)	$T_{s,out}$ = 36 to 52 °F; $T_{s,in}$ = –22 to –8 °F
Total chamber	5809 – 11503 Btu/hr (~1.7 – 3.4 kW)	

Table 7. Simulation Results: Dimensionless Number, Convective, and Overall Heat Transfer Coefficients of Each Section of the Outdoor Climate Chamber

	Inside (Cold) Film Region		Outside (Warm) Film Region	
Ceiling				
Re_{in} =	142 – 146		Re_{out} =	100 – 103
Ra_{in} =	$(8.99 – 16.4) \cdot 10^9$		Ra_{out} =	$(3.48 – 7.37) \cdot 10^9$
Nu_{in} =	83 – 97		Nu_{out} =	65 – 79
h_{in} =	0.197 – 0.232 Btu/hr-ft^2-°F (1.12 – 1.32 W/m^2-°C)		h_{out} =	0.188 – 0.223 Btu/hr-ft^2-°F (1.07 – 1.27 W/m^2-°C)
$U_{ceiling}$=	0.025 – 0.06 Btu/hr-ft^2-°F (0.16 – 0.33 W/m^2-°C)			
Floor				
Re_{in} =	151 – 151		Re_{out} =	N/A
Ra_{in} =	$(0.11 – 0.23) \cdot 10^9$		Ra_{out} =	N/A
Nu_{in} =	27.8 – 33.1		Nu_{out} =	N/A
h_{in} =	0.065 – 0.077 Btu/hr-ft^2-°F (0.37 – 0.44 W/m^2-°C)		h_{out} =	N/A
$U_{floor} \leq$	0.0001 Btu/hr-ft^2-°F (0.0007 W/m^2-°C) (adiabatic boundary on the outside surface)			
External wall				
Re_{in} =	$(47 – 48) \cdot 10^3$		Re_{out} =	337 – 345
Ra_{in} =	$(396 – 671) \cdot 10^9$		Ra_{out} =	$(159 – 311) \cdot 10^9$
Nu_{in} =	216 – 243		Nu_{out} =	172 – 200
h_{in} =	0.153 – 0.176 Btu/hr-ft^2-°F (0.87 – 1.0 W/m^2-°C)		h_{out} =	0.15 – 0.17 Btu/hr-ft^2-°F (0.83 – 0.96 W/m^2-°C)
U_{wall} =	0.024 – 0.05 Btu/hr-ft^2-°F (0.14 – 0.29 W/m^2-°C)			
Separation Wall				
Re_{in} =	$(47 – 48) \cdot 10^3$		Re_{out} =	$(34 – 35) \cdot 10^3$
Ra_{in} =	$(375 – 637) \cdot 10^9$		Ra_{out} =	$(158 – 311) \cdot 10^9$
Nu_{in} =	213 – 240		Nu_{out} =	170 – 202
h_{in} =	0.151 – 0.176 Btu/hr-ft^2-°F (0.87 – 1.0 W/m^2-°C)		h_{out} =	0.14 – 0.17 Btu/hr-ft^2-°F (0.82 – 0.95 W/m^2-°C)
$U_{wall,,sep}$ =	0.023 – 0.05 Btu/hr-ft^2-°F (0.13 – 0.27 W/m^2-°C)			

batic as mentioned in the previous section. Thus, the dimensionless numbers and convective heat transfer coefficients do not have a physical meaning in this section (N/A in Table 7). Figure 4 shows the temperature profile in the wall and in the film regions if the interior temperature is at –40°F (–40°C) and the effective thermal conductivity of the panels is about $k_{c,eff}$=0.234 Btu-in/hr-ft^2-°F (0.034 W/m-°C). The temperature profile in the film regions were calculated according to the laminar convection boundary theory [34] and they are plotted versus the x-coordinate, which is the direction perpendicular to the surface of the panel. If the panel thickness, t_{panel}, varies from 2 to 6 inches then its thermal insulation between ambient and interior of the chamber augments. The temperature in the inside and outside surfaces increases and the heat transfer rate gained into the outdoor chamber from the ambient decreases from about 11503 to 5809 Btu/hr (~3.4 to 1.7 kW).

The temperature on the outside surface is higher than the dew point of the ambient only if the panel thickness reaches about 5 inches (12.7 cm) as shown in Figure 4 and more in details in Figure 5. For this thickness, the heat transfer rate from the surrounding to the interior of the chamber is about 6612 Btu/hr (~1.9 kW). If the panel side width varies from 3 and 8 ft, the effective thermal conductivity changes of about ±10% from the average value $k_{c,eff}$ due to the thermal bridge effect of the metal sheet sides. This variation of effective thermal conductivity leads to a temperature variation of the outside surface of about ±1.2°F (±0.67°C) as shown by the y-error bar in Figure 5.

From the panel manufacturer point of view, the highest thickness of a single panel that can be made using conventional tools is about 4 inches (10.2 cm). A thicker panel would require special tools and equipment and it would penalize tremendously the cost of manufacturing. While a 5 inch deep panel would prevent condensation at –40°F (–40°C), a 4 inch panel with similar thermal insulation characteristics would be sufficient to prevent water vapor condensation on the outside surfaces if the interior temperature is as low as –20°F (–28.9°C), as shown in the parametric study of Figure 6. The temperature of the outside wall surface is plotted versus the thickness of the panel at different interior temperature ranging from –40 to 0°F (–40 to –17.8°C). The results from the parametric study indicate that in the lower temperature ranges (below –20°F) the panel thickness should be between 4 and 5 inches to prevent condensation on the outside surfaces. However, even with a 5-inch thick panel, Figure 7 shows that the temperature of the surface facing the indoor environmental room is lower than the dew point temperature of the air inside that room, which is about 54°F (12.2°C). This means that droplets of water vapor condensate are expected to form at the surface of the intermediate wall that separate the outdoor from indoor chamber.

It is expected that the outdoor climate chamber at Oklahoma State University will actually operates above –20°F for most of its life time, achieving –40°F for only few tests and for short periods of time. Thus, a panel thickness of about 4 inches represents a trade off between excellent thermal insulation, feasibility of production, and cost of manufacturing of the structure. For the separation intermediate structure between the outdoor and indoor room, a double panel wall should be provided and a mean to properly collect water vapor condensate, which forms drops on the surface, should be designed for this section.

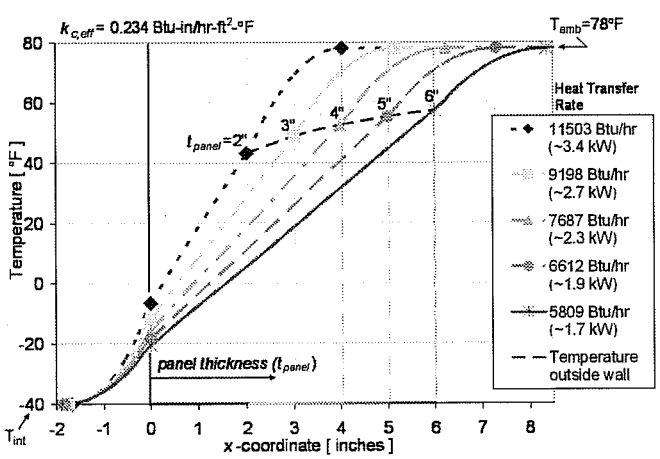

Figure 4 *Temperature profiles in the direction perpendicular to the wall surface of the outdoor climate chamber (interior temperature at –40°F (–40°C) and average effective thermal conductivity of the panels of 0.234 Btu-in/hr-ft^2-°F (0.034 W/m-°C)).*

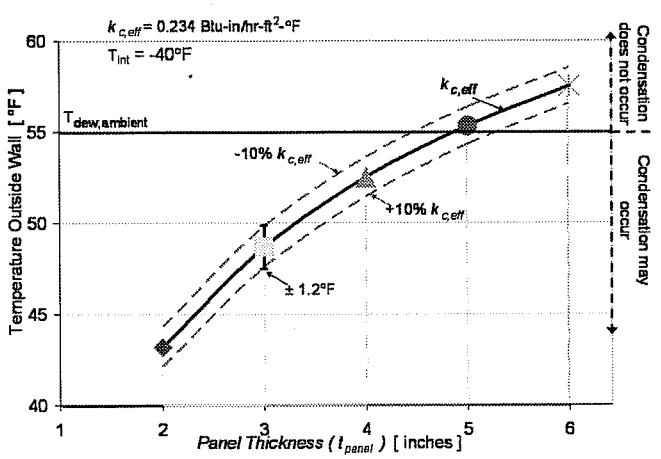

Figure 5 *Temperature of the outside wall surface of the outdoor climate chamber versus wall panel thickness (t_{wall}) (interior temperature at –40°F (–40°C) and average effective thermal conductivity of the panels of 0.234 Btu-in/hr-ft^2-°F (0.034 W/m-°C)).*

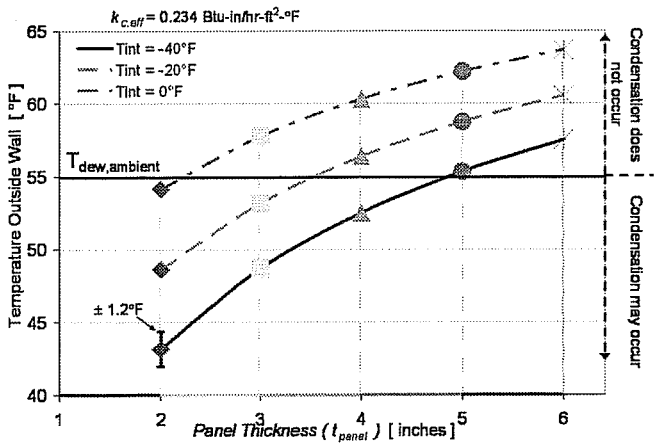

Figure 6 *Temperature of the outside wall surface of the outdoor climate chamber versus wall panel thickness (t_{wall}) at different interior temperatures (average effective thermal conductivity of the panels of 0.234 Btu-in/hr-ft²-°F (0.034 W/m-°C)).*

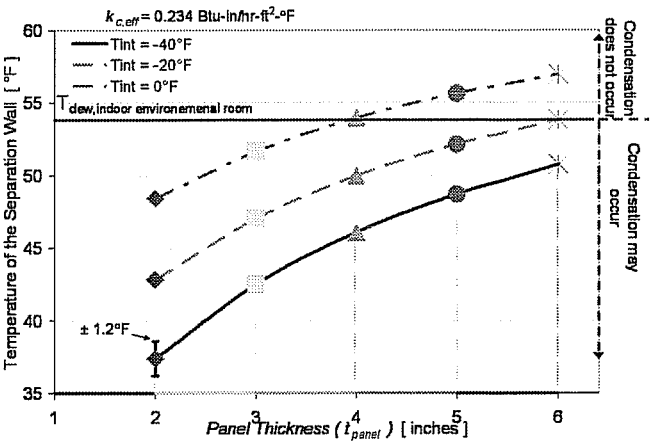

Figure 7 *Surface outer temperature of the separation wall of the outdoor climate chamber versus wall panel thickness (t_{wall}) at different interior temperatures (average effective thermal conductivity of the panels of 0.234 Btu-in/hr-ft²-°F (0.034 W/m-°C)).*

Air leak infiltration is not considered in the present heat transfer analysis and it should be taken into account in further refinement and optimization of the structure. In this preliminary calculation, it is assumed that the chamber is leak tight but a safety factor can added to the heat transfer rate to account for air leak infiltration. The cooling capacity of the refrigeration system of the facility should be oversized of about 1 tons of refrigeration (12,000 Btu/hr) at air temperature of –40°F. This additional capacity would compensate the heat gain from the surrounding to the chamber for operating temperature below freezing, which reaches a maximum of about 7687 Btu/hr (~0.6 tons) for a 4 inches panel.

SUMMARY AND CONCLUSIONS

A design and heat transfer analysis of a psychrometric chamber for low temperature heat pump and refrigeration system testing is presented. The facility consists of a structure of dimensions of about 42 by 22 by 17 ft high (13 x 7 x 5m) and it is divided in two nearly-identical rooms: one is used for the outdoor climate chamber and the other is used for the indoor environmental simulator. The outdoor climate chamber temperature varies between –40° to 130°F (–40° to 54.4°C) and the relative humidity ranges from 10 to 95% RH. In these extreme conditions, it was found that the existing knowledge available in the open literature was not sufficient to provide complete information for the design of the psychrometric facility. During the early stage design phase decisions must be made about size, material, configuration, and capacity of the structure and of the conditioning equipment in relation to the capacity and size of testing equipment inside the chamber. Thus, a heat transfer model was developed using a control volume approach for the structure of the chamber. The current model, which was validated against results from the literature, is simple but accurate enough to be useful in practice engineering and it provides initial values for finite-element and CFD numerical heat transfer models that can be used for further refinement and optimization. The present model estimated the heat transfer gained from the surrounding into the chamber and calculate the panel thickness that would prevent water vapor condensation on the outside surfaces of the psychrometric facility. From the heat transfer analysis of the present work, it is concluded that the psychrometric chamber have to be made of panels of at least 4 inches thick and their effective thermal conductivity needs to be less or equal to 0.234 Btu-in/hr-ft²-°F (0.034 W/m-°C). This can be achieved by using the enhanced insulation expanded foams available in the market and by manufacturing large panels to minimize the thermal bridge effect. If the interior of the chamber is at –40°F (–40°C), the heat transfer gained from the surrounding into the chamber is about 7687 Btu/hr (~2.3 kW). The cooling capacity of the refrigeration system for this psychrometric facility should be oversized of about 1 tons of refrigeration (12,000 Btu/hr) at air temperature of –40°F. This additional capacity compensates for the heat transfer gain from the surrounding into the outdoor climate chamber when it operates below freezing temperature.

ACKNOWLEDGMENTS

The authors would like to gratefully acknowledge the help of AAON, Inc. and the support from the College of Engi-

neering, Architecture and Technology at the Oklahoma State University.

REFERENCES

[1] DOE, "Code of Federal Regulation," 1-1-06 ed, D. o. Energy, Ed.: US Government Printing office, 2006.

[2] Y. Hwang, L. Cremaschi, R. Radermacher, T. Hirata, Y. Ozaki, and T. Hotta, "Oil circulation behavior in low temperature CO_2 climate control systems," in *SAE World Congress*, Detroit, USA, 2004, pp. 33-38.

[3] Y. Hwang, J. Dae-Hyun, and R. Radermacher, "Comparison of hydrocarbon R-290 and two HFC blends R-404A and R-410A for low temperature refrigeration applications," University of Maryland, College Park, MD, USA, Final Report prepared for International Council of Air-Conditioning and Refrigeration Manufacturer's Associations and Air-Conditioning and Refrigeration Institute, Nov. 17, 2005.

[4] C. Y. Park and P. S. Hrnjak, "CO_2 and R410A flow boiling heat transfer, pressure drop, and flow pattern at low temperatures in a horizontal smooth tube," *International Journal of Refrigeration,* vol. 30, pp. 166-178, 2007.

[5] G. R. Smith, "Latent heat, equipment-related load, and applied psychrometrics at freezer temperatures," in *ASHRAE Transactions*, Anaheim, CA, USA, 1992, pp. 649-657.

[6] P. J. Mago, N. K. Al-Mutawa, R. S. Theen, K. Bilen, S. A. Sherif, and R. W. Besant, "Psychrometrics in the supersaturated frost zone," in *ASHRAE Transactions*, Cincinnati, OH, 2001, pp. 753-767.

[7] N. Aljuwayhel, F., Reindl, D., T., Klein, S., A., and Nellis, G., F., "Simple method to improve the performance of industrial evaporator under frosting conditions," in *International Refrigeration and Air Conditioning Conference at Purdue*, Purdue University, West Lafayette, IN, 2006, p. 8.

[8] S. K. Chatzidakis and K. S. Chatzidakis, "Refrigerated transport and environment," *International Journal of Energy Research,* vol. 28, pp. 887-897, 2004.

[9] ARI, "ARI Standard 210/240-2005, Unitary air conditioning and air-source heat pump equipment," ARI, Ed., 2005.

[10] ARI, "ARI Standard 340/360-2004, Commercial and industrial unitary air-conditioning and heat pump equipment," ARI, Ed., 2004.

[11] D. C. Price, P. Townsend, M. C. Woods, W. G. Wyatt, and B. W. Fennell, "Design of a transient, temperature control system for a low-temperature infrared optical teelescope utilizing a ramai R-cooled thermoelectric assembly as the condenser of a two-phase cooling system," in *Proc. of the ASME/Pacific Rim Technical Conference and Exhibition on Integration and Packaging of MEMS, NEMS, and Electronic Systems: Advances in Electronic Packaging 2005*, San Francisco, CA, United States, 2005, pp. 683-696.

[12] J. A. Manzione and F. E. Calkins, "Improved performance of transcritical carbon dioxide as a refrigerant in army tactical environmental control units," in *Proc. of the ASME Conference, Advanced Energy Systems Division (Publication) AES*, New York, NY, United States, 2001, pp. 269-274.

[13] Y. R. Mehra, "How to estimate power and condenser duty for ethylene refrigeration systems," *Chemical Engineering (New York),* vol. 85, pp. 97-104, 1978.

[14] ASHRAE, "ANSI/ASHRAE 37-1988, Method of testing for rating unitary air conditioning and heat pump equipment. ," ASHRAE, Ed., 1988.

[15] ASHRAE, "ANSI/ASHRAE 41.2-1987, Standard methods for laboratory airflow measurement," ASHRAE, Ed., 1987.

[16] ASHRAE, "ANSI/ASHRAE 41.1-1986, Standard method for temperature measurement," ASHRAE, Ed., 1986.

[17] ASHRAE, "ANSI/ASHRAE 40-1980, Methods of testing for rating heat-operated unitary air-conditioning equipment for cooling. ," ASHRAE, Ed., 1980.

[18] B. N. Taylor and C. E. Kuyatt, "Guidelines for evaluating and expressing the uncertainty of NIST measurement results," 1994 ed. vol. 20: U.S. Dept. of Commerce, Technology Administration, National Institute of Standards and Technology, Gaithersburg, MD, USA, 1994, p. 28 cm.

[19] T. J. Herrmann, J. S. Zhang, Z. Zhang, J. Smith, X. Gao, H. Li, W. Chen, and S. Wang, "Performance test results for a large coupled indoor/outdoor environmental simulator (C-I/O-ES)," in *ASHRAE Transactions*, Kansas City, MO, United States, 2003, pp. 503-516.

[20] K. C. Karki and S. V. Patankar, "Airflow distribution through perforated tiles in raised-floor data centers," *Building and Environment,* vol. 41, pp. 734-744, 2006.

[21] S. V. Patankar and K. C. Karki, "Distribution of cooling airflow in a raised-floor data center," in *2004 Annual Meeting - ASHRAE Technical and Symposium Papers*, Nashville, TN, United States, 2004, pp. 599-603.

[22] F. S. Bauman, L. P. Johnston, H. Zhang, and E. A. Arens, "Performance testing of a floor-based, occupant-controlled office ventilation system," in *ASHRAE Transactions*, New York, NY, USA, 1991, pp. 553-565.

[23] F. S. Bauman, E. A. Arens, S. Tanabe, H. Zhang, and A. Baharlo, "Testing and optimizing the performance of a floor-based task conditioning system," *Energy and Buildings,* vol. 22, p. 173, 1995.

[24] S. K. Chatzidakis, A. K. Athienitis, and K. S. Chatzidakis, "A numerical simulation study of a new environmental chamber," in *ASHRAE Transactions*, Honolulu, HI, United States, 2002, pp. 113-118.

[25] M. J. Swedish, "Development of a psychrometric test chamber," in *ASEE Annual Conference Proceedings*, Cahrlotte, NC, United States, 1999, pp. 1769-1775.

[26] F. A. Sando and O. A. Abdou, "Environmental/psychrometric test cells in industrial facilities," *Journal of Architectural Engineering,* vol. 1, pp. 108-114, 1995.
[27] E. Berchtold, "Selecting an environmental test chamber," *Evaluation Engineering,* vol. 43, pp. 20-25, 2004.
[28] K. Barber, "Climatic test chambers - Making an informed decision," *Environmental Engineering,* vol. 14, pp. 46-49, 2001.
[29] D. Crawley, B., Lawrie, L.,K., Pedersen, C.,O. , Liesen, R.,J. , Fisher, D.,E. , Strand, R.,K. , Taylor, R.,D., Winkelmann, R.,C. , Buhl, W.,F., Huang, Y.,J. , and Erdem, A.E., "ENERGYPLUS, A New-Generation Building Energy Simulation Program," in *Proc. Building Simulation'99*, Kyoto, Japan, 1999, pp. 81-88.
[30] SEL, "Solar Energy Laboratory (SEL) TRNSYS, A Transient Systems Simulation Program, User's Manual, Version 14.2," University of Wisconsin-Madison, 1997.
[31] ASHRAE, *2001 ASHRAE Handbook fundamentals.* Atlanta, GA, USA: ASHRAE, 2001.
[32] F. C. McQuiston, J. D. Parker, and J. D. Spitler, *Heating, ventilating, and air conditioning analysis and design*, 6 ed. New York, NJ, USA: John Wiley & Sons, 2005.
[33] A. M. Malkawi, "Developments in environmental performance simulation," *Automation in Construction,* vol. 13, pp. 437-445, 2004.
[34] J. P. Holman, *Heat transfer*, 8 ed. New York, NJ, USA: McGraw-Hill, 1997.
[35] F. P. Incropera and D. P. DeWitt, *Fundamental of heat and mass transfer*, 2 ed. New York, NJ, USA: John Wiley & Sons, 1985.
[36] S. Astling and B. Weber, "Thermal conductivity test rig," Final report submitted to AAON, Inc.; Montana State University, Bozeman, MT, USA, 2005.
[37] S. Peng and A. Fuchs, "Transport modeling and thermophysical properties of cellular poly(urethane-isocyanurate)," *Polymer Engineering and Science,* vol. 41, pp. 484-491, 2001.
[38] S. A. Klein, "Engineering Equation Solver," V7.723-3D ed, Madison, WI, USA: F-Chart Software, 2006.
[39] E. A. Vineyard, T. K. Stovall, K. E. Wilkes, and K. W. Childs, "Superinsulation in refrigerators and freezers," in *ASHRAE Transactions*, Toronto, Can, 1998, pp. 1126-1134.
[40] B. Griffith and D. Arasteh, "Advanced insulations for refrigerator/freezers: the potential for new shell designs incorporating polymer barrier construction," *Energy and Buildings,* vol. 22, pp. 219-231, 1995.
[41] J. K. Gupta, M. Ram Gopal, and S. Chakraborty, "Modeling of a domestic frost-free refrigerator," *International Journal of Refrigeration,* vol. 30, pp. 311-322, 2007.

APPENDIX

The correlations used in the present model are discussed in detail in [34, 35] and they are briefly summarized in this appendix. The characteristic length of the surface is defined as $L = h$ for vertical plates (walls of the chamber), and $L = A_s/P$ for horizontal plates (ceiling and floor of the chamber), where h is the height of the plate, A_s and P are is the plate surface area and perimeter, respectively.

If the ratio Gr/Re^2 is less than 10, then forced convection is the predominant convection type. In this case the Nusselt number is calculated using the following correlation:

$$\overline{Nu} = 0.664 \cdot Re^{0.5} \cdot Pr^{1/3} \quad \text{valid if } Re < 5 \cdot 10^5 \qquad (A.1)$$

If natural (free) convection is the predominant convection type, then for horizontal plate (upper surface cooled plate or lower surface heated plate) the Nusselt number is calculated as follows:

$$\overline{Nu} = 0.27 \cdot Ra^{1/4} \quad \text{valid if } 10^5 < Ra < 10^{11} \qquad (A.2)$$

where $Ra = Gr \cdot Pr$, is the Raleigh number.

If natural (free) convection is the predominant convection type, then for vertical plate the Nusselt number is calculate using the following correlations:

$$\overline{Nu}^{1/2} = 0.825 + \frac{0.387 \cdot Ra^{1/6}}{[1 + (0.492/Pr)^{9/16}]^{8/27}} \quad \text{valid if } 10^{-1} < Ra \le 10^2 \qquad (A.3)$$

$$\overline{Nu} = 0.68 + \frac{0.670 \cdot Ra^{1/4}}{[1 + (0.492/Pr)^{9/16}]^{4/9}} \quad \text{valid if } 10^2 < Ra < 10^9 \qquad (A.4)$$

$$\overline{Nu} = 0.1 \cdot Ra^{1/3} \quad \text{valid if } Ra \ge 10^9 \qquad (A.5)$$